IEEE Access
Multidisciplinary ⋮ Rapid Review ⋮ Open Access Journal

Received March 29, 2021, accepted May 3, 2021, date of publication May 17, 2021, date of current version May 25, 2021.

Digital Object Identifier 10.1109/ACCESS.2021.3080933

A Wideband Channel Model for Body Area Networks in Circular Metallic Indoor Environments

FILIPE D. CARDOSO[1], (Member, IEEE), MANUEL M. FERREIRA[1], SŁAWOMIR J. AMBROZIAK[2], (Senior Member, IEEE), AND LUIS M. CORREIA[3], (Senior Member, IEEE)

[1]ESTSetúbal, Polytechnic Institute of Setúbal and INESC-ID, 2914-508 Setúbal, Portugal
[2]Faculty of Electronics, Telecommunications, and Informatics, Gdańsk University of Technology, 80-233 Gdańsk, Poland
[3]IST/INESC-ID, University of Lisbon, 1000-029 Lisbon, Portugal

Corresponding author: Filipe D. Cardoso (filipe.cardoso@estsetubal.ips.pt)

ABSTRACT In this paper, the wideband characterization of the propagation channel in circular metallic indoor environments is addressed, regarding Body Area Networks and 5G small cells, an analytical model for the dependence of the mean delay and the average delay spread on the circle radius, the working frequency and the distance between the transmitter and the receiver being proposed. The derivation of the model is initially done analytically, based on optical physics, after which simulation results allow to obtain the values of the coefficients. The simulator was previously assessed with measurements at 2.45 GHz in a passenger ferry room with a circular shape. For a random positioning of the transmitter and the receiver, and a given distance between them, it is observed that the mean delay and the delay spread increase linearly with the radius; furthermore, the mean delay increases quadratically with the distance, while the delay spread has a concave parabolic behavior, with the maximum being at a distance equal to the radius. In a practical case, regarding the positioning of an Access Point inside the room, it is recommended that it is done at the circle center, in order to reduce delay spread.

INDEX TERMS Body Area Networks, wideband characterization, circular metallic structures, propagation channel.

I. INTRODUCTION

The rapid development of wireless technologies, together with the emergence of new applications and services in areas such as health monitoring and safety, has driven Body Area Networks (BANs) (i.e., wireless networks operating inside, on or in the proximity of the user's body) and 5G cellular systems (namely, small cells) to be developed in unusual environments, like ships and passenger ferries in order to increase comfort and safety. Due to the specific characteristics of these environments, since walls, floors and ceilings are mostly made of metallic materials for which the reflection coefficient is close to -1, proper models are needed for planning purposes in these scenarios.

There is a large number of studies related to the BAN propagation channel in different environments, e.g., [1]–[3], and especially for medical applications [4], [5]. Most of these studies are based on indoor measurements, such as rooms, corridors and similar environments [6], [7].

There are also some papers describing research on the propagation channel characterization in ships, mostly composed of metallic walls. A path loss model at 2.4 GHz, based on measurements made in two different ferries and three types of rooms (engine room, passengers' deck and vehicles parking) was proposed in [8]. The characterization of a wireless channel at 2.5 GHz in a cruise ship was presented in [9], while in [10] a wideband channel characterization at 255.6 MHz is presented. An empirical study, addressing path loss and delay spread in the range of [0.8, 2.6] GHz (at the machine and engine rooms, and the main starboard hallway) is presented in [11]. Finally, in [12], the electromagnetic environment characterization in the range of [0.1, 10] GHz in two types of below-deck spaces has been presented. Still, all the above-mentioned studies do not account for the specific

The associate editor coordinating the review of this manuscript and approving it for publication was Celimuge Wu.

aspects of BANs, namely the proximity of the user's body to a device.

The current work considers the so-called off-body case, in which one antenna is placed on the user's body and the other is placed in some fixed position in the environment, acting as an access point to the external network. In this kind of BANs, one needs to consider the influence of the body on the wearable antenna's characteristics, the placement of the antenna on the body, the relative motion of the antenna to the user (e.g., when it is mounted on a hand) and the user's motion. One should also take the body shadowing effect into account, in which the user's body may become an obstacle for both the direct and the reflected waves, causing additional fades of the received signal power.

As far as the authors are aware of, the first research on BAN radio channels in metallic environments has been described in [13]. In [14], propagation inside circular metallic structures is addressed and a channel model was proposed and assessed with measurements at 2.45 GHz in a passenger ferry discotheque with an 8 m diameter circular shape. The measurement campaign focused on system loss measurements in the link between a transmitting antenna (Tx) located on the body in different locations and a receiving one (Rx) positioned off-body. Different walking scenarios have been considered, allowing to perform the analysis of system loss for various conditions, including different on-body antenna placements. Based on the results from this measurement campaign, a fading analysis was performed, fast fading statistical distribution parameters being derived. These previous studies were focused on path-loss and fading analysis, hence, no temporal parameters of the propagation channel were extracted and modeled.

Wideband temporal parameters of the propagation channel for BANs in different frequency bands and covering a huge range of environments and applications have already been studied in the past, e.g., [15]–[17]. Still, there are no known studies for BANs in indoor metallic environments as the ones being addressed in this paper, i.e., circular ones.

In the current paper, the model in [14] is used to address the temporal characteristics of the propagation channel as a function of the radius of the circular environment, and an analytical model for the dependence of mean delay and average delay spread on the radius, the working frequency and the distance between an Access Point (AP) and a Mobile Terminal (MT) is proposed (obviously, either can serve as both Tx and Rx). One should remember that the circular shape has some specific characteristics (catacaustic regions) not found in usual environments with other geometries, namely rectangular ones, such as rooms and corridors, its analysis being one of the novelties of this paper.

Given the two-dimensional approach to the problem, the position of the antennas on the body is not relevant. As mentioned in [14], the objective is to keep the model as simple as possible, while still being accurate enough to describe reality and keeping the deviation from measurements within an acceptable margin. Naturally, this simple model has limitations, namely when different antennas heights are considered. Additionally, in a real scenario, walls are not perfect conducting flat boundaries, having impact on the values of the reflection coefficient. Moreover, among other aspects, the scenario dynamics, namely due to the presence of people and obstacles, the use of different types of antennas/polarizations and the user's body movement (causing antennas misalignment), will also have an impact on results. Still, among all these limitations, the proposed model allows to reasonably match the results from measurements for the conditions under study [14]. The three-dimensional approach is left for future work.

This paper is organized as follows. The propagation channel model for circular environments with metallic walls is presented in Section II. A description of the simulator implementing the model and of results for the average mean delay and delay spread is done in Section III. The wideband channel model resulting from this analysis is proposed in Section IV. Conclusions are drawn in Section V.

II. MODEL DESCRIPTION

The scenario is a circular structure of radius r with perfect conducting walls, with a Tx at given point T inside the circle and an Rx at a point R also inside the circle, with a distance d between the two. Many reflections exist between Tx and Rx, depending on their relative positioning, an example with 4 reflections of 1st order being illustrated in Figure 1.

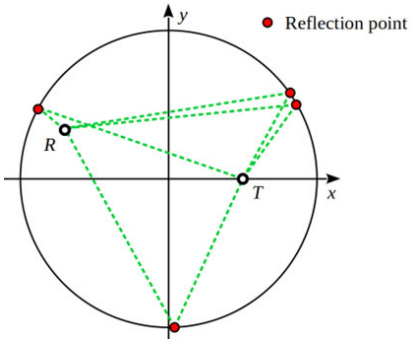

FIGURE 1. Reflection inside a circle [14].

In this scenario, the reflection coefficient can be considered to be -1, thus, the amplitude of the reflected components is of the same order of magnitude of the LoS (Line-of-Sight) one, the main difference being only due to the different path lengths. The signal at the Rx can be described by the sum of the LoS component with the reflected ones; many reflections are observed, their importance decreasing for an increasing reflection order, due to the increasing path length and the corresponding increasing attenuation. Regions with a given number of reflections are defined as catacaustic zones [18], [19, p. 183-186], Figure 2 showing the catacaustic regions for different Rx positions, when 1st and 2nd order reflections are considered: 2 or 4 reflections are observed for 1st order reflections, while for 2nd order ones, one can see that there are up to 8, [14].

When analyzing the sum of the reflection components, one can consider up to N_r order reflections, with R_m reflected rays in each one, hence, the signal at the Rx is described by [14],

$$E_{N_r} = \sum_{m=0}^{N_r} \sum_{n=1}^{R_m} E_{mn} \tag{1}$$

with E_{mn} corresponding to the received electric field of the n^{th} reflected ray of the m^{th} reflection order ($m = 0$ corresponds to LoS), being given by

$$E_{mn} = \frac{\sqrt{30P_t}}{d_{mn}} \Gamma^m e^{-j\frac{2\pi d_{mn}}{\lambda}} \tag{2}$$

where:

- Γ^m : reflection coefficient of the m^{th} reflection order, being $(-1)^m$;
- λ : wavelength;
- d_{mn} : path length of the n^{th} reflected ray of the m^{th} reflection order;
- P_t : Tx power.

In the above, one is assuming that both the Tx and the Rx have isotropic antennas and that the dimensions of the environment are large enough compared to the wavelength, so that plane waves can be considered at the Rx. The consideration of other types of antennas can be easily implemented by introducing in (2) a function accounting for the radiation patterns, e.g., as in [20], but this is left for future work, so that in the current one the aspects related to the propagation channel are isolated and understood, without the antennas' influence; additionally, AP's antennas are fairly omnidirectional and MTs' can be approximately as such as well, therefore, this approximation is acceptable.

The Power Delay Profile (PDP) can then be obtained from (2) as [21, p. 185],

$$\mathrm{P}(\tau) = \sum_{m=1}^{N_r} \sum_{n=1}^{R_m} \frac{A}{d_{mn}^2} \cdot \delta\left(\tau - \tau_{mn}\right) \tag{3}$$

where:

- A : a normalized amplitude,
- τ_{mn} : relative delay associated to the path length of the n^{th} reflected ray of the m^{th} reflection order compared to the direct path between Tx and Rx, which can be expressed by

$$\tau_{mn} = \frac{d_{mn} - d}{c} \tag{4}$$

where c is the speed of light.

Given the geometry of the problem, for any given positions of the Tx and the Rx, d_{mn} is finite for any reflection order and limited by multiples of the diameter, as is d, so that

$$d_{mn} = \alpha_{mn} r \tag{5}$$

with

$$0 < \alpha_{mn} < 2(m+1) \tag{6}$$

(the equality in (6) in either sides would exist only when the Tx and the Rx are superimposed), and

$$d = \gamma r \tag{7}$$

with

$$0 < \gamma \leq 2 \tag{8}$$

(the lower equality in (8) would exist only when the Tx and the Rx are superimposed, and the upper one corresponds to the Tx and the Rx positioned in the opposite ends of a diameter).

The calculation of α_{mn} (which is only geometrical dependent) is not analytically tractable, given the complexity of the analytical solutions for the location of the reflection points at the circumference for a given position of the Tx and the Rx, [18], but the relationship in (5) allows one to establish a relationship of proportionality with the size of the environment, i.e., r. In the case of γ, its calculation is obviously a simple one, once the positions of the Tx and the Rx are known. It should be noted that since a reflected wave has a path always larger than the direct one, the following inequality applies

$$\alpha_{mn} - \gamma > 0 \tag{9}$$

Taking the definitions of the mean delay τ_m and of the delay spread σ_τ [21, p. 186], with some algebraic manipulation one gets

$$\tau_m = (S_\tau / f)(r/\lambda) \tag{10}$$

$$\sigma_\tau = (S_\sigma / f)(r/\lambda) \tag{11}$$

where:

- f : frequency,
- S_τ : proportionality factor for τ_m, given by

$$S_\tau = \frac{\sum_{m=1}^{N_r} \sum_{n=1}^{R_m} \frac{\alpha_{mn} - \gamma}{\alpha_{mn}^2}}{\sum_{m=1}^{N_r} \sum_{n=1}^{R_m} \frac{1}{\alpha_{mn}^2}} \tag{12}$$

- S_σ : proportionality factor for σ_τ, given by

$$S_\sigma = \sqrt{\frac{\sum_{m=1}^{N_r} \sum_{n=1}^{R_m} \left(\frac{\alpha_{mn} - \gamma - S_\tau}{\alpha_{mn}}\right)^2}{\sum_{m=1}^{N_r} \sum_{n=1}^{R_m} \frac{1}{\alpha_{mn}^2}}} \tag{13}$$

The assumptions taken for this model are approximations, but they still hold in many practical cases, thus, the simple proportionality in the relationships obtained in (10) and (11) can serve as a good design trend for system deployment.

III. CHANNEL SIMULATION

Given the non-tractability of the analytical solution, the approach to obtain results has to be taken via simulation. The simulator used in this work is an extension of the one used in [14], which allows to evaluate the received signal at any given location inside a circle with perfect conducting boundaries

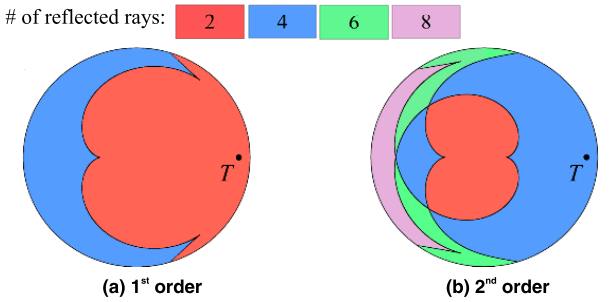

FIGURE 2. Catacaustic regions for 1st and 2nd order reflections [14].

for any position of the Tx. This simulator was assessed with measurements at 2.45 GHz in a circular room (a discotheque in a passenger ferry) with metallic walls and ceiling, and an 8 m radius; the measurements were performed for typical situations occurring for BANs in off-body communications and on-body antenna placements. It was observed that the simulator provides a reasonable accuracy by considering reflections up to the 2nd order.

In order to properly characterize the propagation channel, the PDP (with delays relative to the LoS path, as expressed in (4)) was obtained for values of $r/\lambda \in \{33, 49, 66, 82, 98\}$, roughly corresponding to $r \in \{4, 6, 8, 10, 12\}$ m, respectively, for the frequency being considered (2.45 GHz). For each value of r/λ, 5 000 Tx-Rx positions randomly distributed inside the circular area were evaluated.

An example of a PDP in the 2 reflections zone with an 8 m radius and a distance of 3 m between Tx and Rx is illustrated in Figure 3.

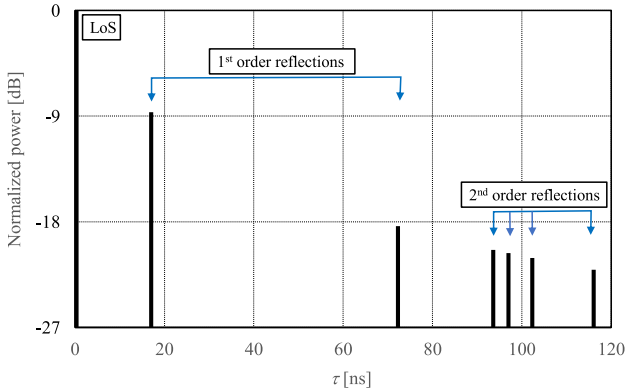

FIGURE 3. Example of a PDP in the 2 reflections zone.

One can see that 7 rays exist in this case, corresponding to 2 reflections of the 1st order, 4 of the 2nd order and the LoS component. It should be noted that, for simplicity, in what follows, when referring to the 2 and 4 reflections zones, one is referring to the ones corresponding to the 1st order reflections case, which corresponds on average to two different zones where a higher or a lower number of reflections is observed when both 1st and 2nd order reflections are considered.

The simulation process was implemented as follows. At each Tx-Rx position, τ_m and σ_τ were evaluated from the obtained PDPs, the values for the average and for the standard deviation of these two parameters taken over all positions, $\overline{\tau_m}$, σ_{τ_m}, $\overline{\sigma_\tau}$, σ_{σ_τ}, being presented in Table 1.

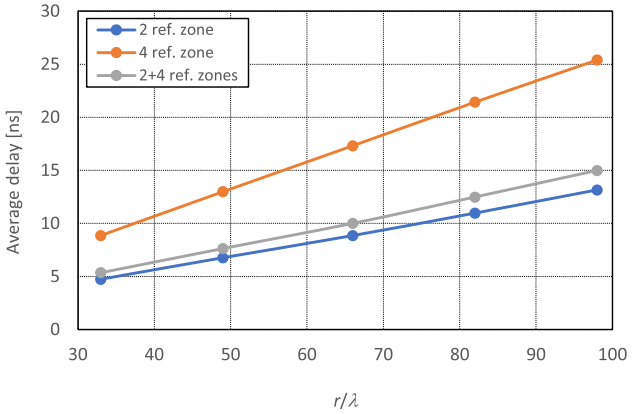

FIGURE 4. Dependence of $\overline{\tau_m}$ as a function of r/λ.

TABLE 1. Average and standard deviation of mean delay and delay spread for 2, 4 and 2+4 reflections zones.

Zone	r/λ	τ_m		σ_τ	
		$\overline{\tau_m}$ [ns]	σ_{τ_m} [ns]	$\overline{\sigma_\tau}$ [ns]	σ_{σ_τ} [ns]
2	33	4.733	1.705	10.470	1.629
	49	6.760	2.700	15.384	2.831
	66	8.851	3.708	20.402	4.098
	82	10.967	4.690	25.378	5.316
	98	13.162	5.639	30.447	6.477
4	33	8.855	0.924	9.977	0.921
	49	12.990	1.801	14.767	1.502
	66	17.321	2.263	19.674	1.994
	82	21.426	2.895	24.618	2.465
	98	25.396	3.842	29.359	2.970
2 and 4	33	5.357	2.186	10.396	1.553
	49	7.634	3.376	15.298	2.693
	66	10.004	4.584	20.303	3.887
	82	12.484	5.795	25.268	5.011
	98	14.985	6.946	30.285	6.096

The variation of $\overline{\tau_m}$ as a function of r/λ in the several reflections zones is shown in Figure 4, while the one of $\overline{\sigma_\tau}$ is presented in Figure 5.

As expected, $\overline{\tau_m}$ shows a linear dependence on r/λ, as shown in (10). Regarding the dependence on the different zones, it is observed that the values of $\overline{\tau_m}$ in the 2 reflections zone are close to the ones obtained when both zones are considered, while in the 4 reflections zone this variation is higher with the latter being around twice of the former. It should be stressed that, besides depending on the relative positioning of the Tx and Rx, the 4 reflections zone is always smaller than the 2 reflections one, the total area where 4 reflections are observed being only 13.4% of the whole circle area [14].

As expected as well, from (11), $\overline{\sigma_\tau}$ shows a linear dependence on r/λ. It should be noted that no dynamic range constraint was taken in simulations, hence the calculation of $\overline{\tau_m}$ and $\overline{\sigma_\tau}$ has no limitation on the difference among the powers of the several contributions; in a real situation, where

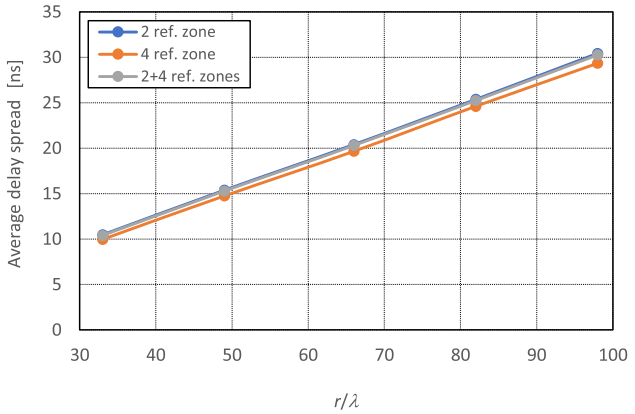

FIGURE 5. Value of $\overline{\sigma_\tau}$ as a function of r/λ.

receivers are limited by a given dynamic range and sensitivity, one could expect small deviations from the shown results. For the cases under study, the dynamic range of the simulated PDPs varies between 39.6 dB and 47.0 dB, respectively, for the extreme values of r/λ equal to 33 and 98, respectively, which is quite acceptable for actual receivers.

Concerning the dependence on the different reflection zones, it is observed that $\overline{\sigma_\tau}$ is almost independent of these zones. The absolute values can be considered low (the maximum for the studied scenarios is 30 ns) compared with the ones that are observed in harsh urban scenarios (in the order of 1 μs), but still it should be taken into account if quite high data rates are aimed at.

In order to model the behavior of $\overline{\tau_m}$ and $\overline{\sigma_\tau}$, while keeping it as simple as possible, one considers both regions altogether, which corresponds to 86.6% of the possible Tx-Rx locations, and takes the linear dependence as mentioned before, leading to (from fitting the obtained results)

$$\overline{\tau_m}_{[\text{ns}]} = 0.148 \cdot \frac{r}{\lambda} + 0.393 \tag{14}$$

$$\overline{\sigma_\tau}_{[\text{ns}]} = 0.305 \cdot \frac{r}{\lambda} + 0.295 \tag{15}$$

The standard deviations of these parameters, σ_{τ_m} and σ_{σ_τ}, also show an almost linear behavior with r/λ. Their values are similar for a given r/λ, being around half of the averages, which shows that the averages can be comfortably taken for system design and deployment.

IV. MODELING OF TIME DISPERSION PARAMETERS

In order to further model the wideband characteristics of the propagation channel in a circular scenario, this section addresses the dependence of both τ_m and σ_τ in terms of both r/λ and d/r, an analytical formulation being proposed. For this purpose, again 5 000 Tx-Rx random positions were evaluated, and in general terms one has observed that both parameters show a second order polynomial dependence on d/r.

An illustration of the dependence of τ_m on d/r is presented in Figure 6. As expected, τ_m tends to increase with d/r, although a significant variation is observed, since for a given

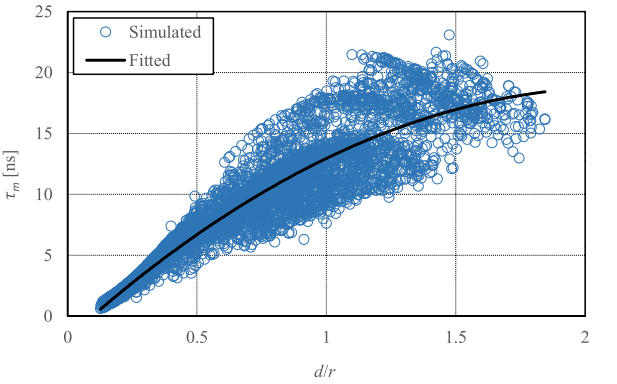

FIGURE 6. Dependence of τ_m on d/r, for $r/\lambda = 66$.

d/r different PDPs are obtained depending on the relative Tx-Rx positioning inside the circle, i.e., a different number of arriving waves can be observed together with varying delays among them. Still, one can consider that the average dependence of τ_m on d/r can be reasonably modeled by a second order polynomial, the coefficient of determination [22, p. 546] being $R^2 = 0.830$, which is quite good for this problem.

A similar approach was followed for σ_τ, as illustrated in Figure 7.

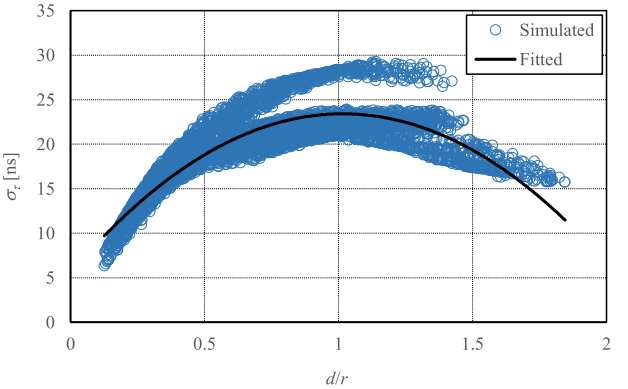

FIGURE 7. Dependence of σ_τ on d/r, for $r/\lambda = 66$.

One can see that σ_τ can also be modeled by a second order polynomial, still, with a different behavior, depending on the number of reflections in the different zones, i.e., with the full concave parabolic dependence over the whole range of d/r.

A more detailed analysis has been done on the delay spread, not only due to its importance in system design but also because of its behavior. Figure 8 shows an example of the several reflection zones, differently colored according to the number of arriving waves (the reflected components plus the LoS one). It is observed that higher values of σ_τ are obtained in locations where the PDP is composed of 7 arriving waves, but the number of Tx-Rx locations where this occurs corresponds to 33.8% of all possible ones, and among them the ones where the highest values of σ_τ are observed being associated with the zone with only 7 arriving waves correspond to only 11.3% of all possible locations. Hence, one considers that σ_τ can be also modeled by a second order

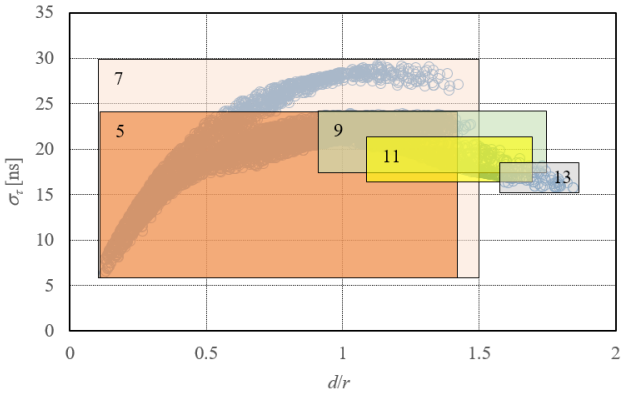

FIGURE 8. Reflection zones for σ_τ as a function of d/r, for $r/\lambda = 66$.

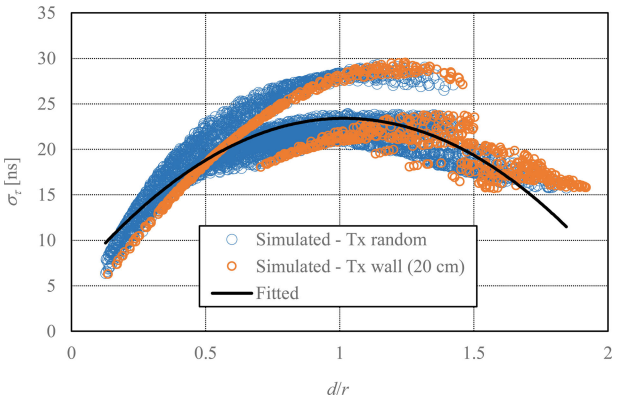

FIGURE 9. Dependence of σ_τ on d/r, for $r/\lambda = 66$ with the AP on the wall.

TABLE 2. Coefficients for the Analytical model of mean delay and delay spread.

r/λ	τ_m			σ_τ		
	a_2	a_1	a_0	a_2	a_1	a_0
33	-2.198	9.961	-0.997	-8.322	16.511	3.382
49	-3.421	14.576	-1.355	-12.722	25.624	4.544
66	-4.475	19.201	-1.785	-17.334	35.202	5.539
82	-5.541	23.561	-2.063	-21.690	44.281	6.677
98	-6.754	28.231	-2.453	-25.890	53.019	7.967

polynomial as presented in Figure 7, having $R^2 = 0.714$, which is still quite acceptable.

An analytical model for τ_m and σ_τ has then been derived from the fitted curves,

$$(\tau_m, \sigma_\tau)_{[\text{ns}]} = a_2 \left(\frac{d}{r}\right)^2 + a_1 \frac{d}{r} + a_0 \tag{16}$$

with the corresponding coefficients presented in Table 2.

Nevertheless, for system design, the approach is to have an AP at a given position, while the MT is indeed at a random position inside the circle. Hence, one has considered two different locations for the AP: on the wall (20 cm away from it, to approximate an actual installation) and at the circle center, results being shown in Figure 9 and Figure 10, respectively. It is clear that the position of the AP at the center leads to a lower delay spread (thus, higher coherence bandwidth), where also the concave parabolic behavior is

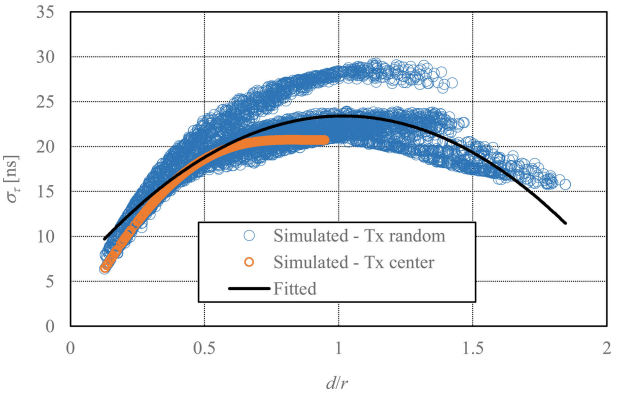

FIGURE 10. Dependence of σ_τ on d/r, for $r/\lambda = 66$ with the AP at the center.

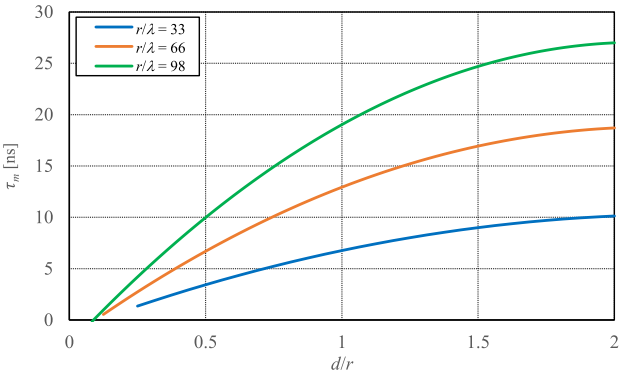

FIGURE 11. Dependence of τ_m on d/r, for several cases of r/λ, with the AP at the center.

better approximated, hence, further modeling effort was performed for this situation, by including the dependence on r/λ. A similar conclusion was reached in [14] regarding fast fading effects. Furthermore, when the AP is on the wall the average distance to random positions of the MT is $d = 1.132r$, while for the AP at the center this average is $d = 0.667r$, which leads to a slightly lower delay spread.

From Table 2, one observes that, in all situations, the coefficients vary linearly with r/λ, hence, a further fitting process was implemented, leading to an excellent coefficient of determination for all cases ($R^2 = 1.000$). The full analytical model for τ_m and σ_τ in terms of both r/λ and d/r is then

$$\tau_{m[\text{ns}]} = -\left(0.069\frac{r}{\lambda} + 0.041\right)\left(\frac{d}{r}\right)^2 + \left(0.279\frac{r}{\lambda} + 0.786\right)\frac{d}{r} - \left(0.022\frac{r}{\lambda} + 0.273\right) \tag{17}$$

$$\sigma_{\tau[\text{ns}]} = -\left(0.271\frac{r}{\lambda} + 0.559\right)\left(\frac{d}{r}\right)^2 + \left(0.562\frac{r}{\lambda} - 1.968\right)\frac{d}{r} + \left(0.069\frac{r}{\lambda} + 1.075\right) \tag{18}$$

The result of this model, for several cases of r/λ, is presented in Figure 11 and Figure 12. It can be seen that τ_m has the maximum for $d/r = 2$, while the maximum of σ_τ occurs for $d/r = 1$ (numerically, it is not exactly at these values, but it is very close to them).

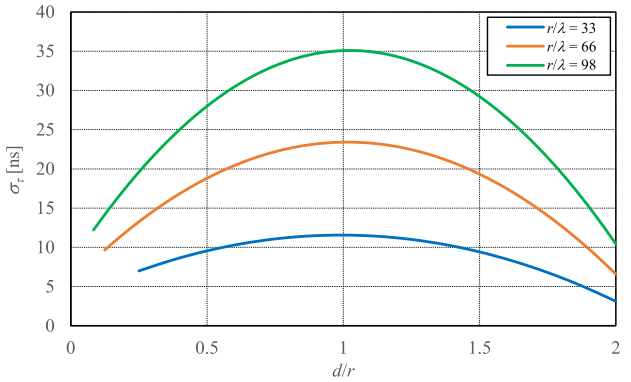

FIGURE 12. Dependence of σ_τ on d/r, for several cases of r/λ, with the AP at the center.

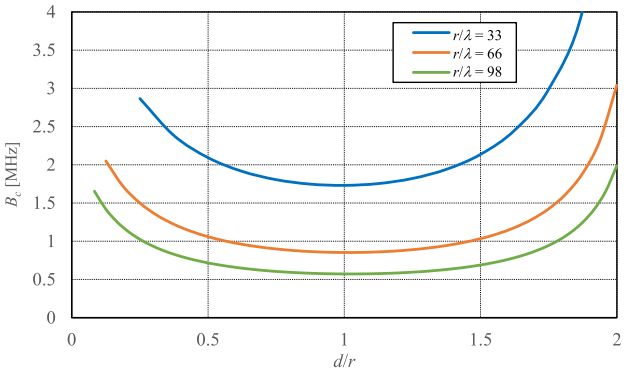

FIGURE 13. Dependence of coherence bandwidth on d/r, for several cases of r/λ, with the AP at the center.

The coherence bandwidth enables to estimate a system behavior for a given channel, which is of interest for system design. For a 90% correlation, the coherence bandwidth can be estimated from [23, p. 163]:

$$B_c = \frac{1}{50\overline{\sigma}_\tau} \tag{19}$$

the resulting dependence on both r/λ and d/r being depicted in Figure 13. The results show that the delay spread's low values lead to a coherence bandwidth of the order of 1 MHz, which is more than enough for most of the systems.

The model proposed above is a simple one, not accounting for many of the random variations in the scenario (such as people's mobility and obstructions by objects), but, still, it leads to a good average estimation on the dependence on the geometrical parameters of the scenario.

V. CONCLUSION

In this paper the wideband channel characteristics of circular metallic indoor environments are addressed. Simulation results were obtained from a simulator that was previously accessed with measurements at 2.45 GHz in a discotheque inside a passenger ferry (an indoor circular environment with a metallic structure both on walls and ceiling). The obtained results were used to derive an analytical model for the dependence of the temporal parameters of the propagation channel, namely mean delay and average delay spread, as a function of the radius of the circular environment, the working frequency and the distance between transmitter and receiver. For a random positioning of the transmitter and the receiver, it is observed that the average values of the mean delay and of the delay spread increase linearly with the increase of r/λ. Concerning the dependence on the distance between the transmitter and the receiver, it is observed that the mean delay increases almost linearly with increasing values of d/r, while the delay spread has a parabolic behavior with a maximum being observed for $d/r = 1$.

In the case that the transmitter is fixed in any given position, e.g., in the case of a fixed Access Point, a different behavior is observed. Two different situations were studied corresponding to transmitter positions close to the wall and at the circle center. It is observed that by positioning the transmitter at the circle center a well-behaved variation is observed with the values of the delay spread being closer to the ones obtained with the analytical model. Hence, from the obtained results, it is proposed that the Access Point should be positioned at the circle center aiming at reducing the delay spread, hence, providing a higher coherence bandwidth, leading to higher data rates of the communication system.

Future work will address the extension to a three-dimensional environment, the inclusion of antennas' radiation patterns, and the consideration of random obstacles inside the scenario.

REFERENCES

[1] *Channel Model for Body Area Network*, Standard IEEE P802.15, Working Group for Wireless Personal Area Networks, New York, NY, USA, 2009.
[2] D. B. Smith, D. Miniutti, T. A. Lamahewa, and L. W. Hanlen, "Propagation models for body-area networks: A survey and new outlook," *IEEE Antennas Propag. Mag.*, vol. 55, no. 5, pp. 97–117, Oct. 2013.
[3] S. J. Ambroziak, L. M. Correia, and K. Turbic, "Radio channel measurements in body-to-body communications in different scenarios," in *Proc. URSI Asia–Pacific Radio Sci. Conf. (URSI AP-RASC)*, Seoul, South Korea, Aug. 2016, pp. 1376–1379.
[4] P. A. Catherwood and W. G. Scanlon, "Link characteristics for an off-body UWB transmitter in a hospital environment," in *Proc. Loughborough Antennas Propag. Conf.*, Loughborough, U.K., Nov. 2009, pp. 569–572.
[5] P. Cui, Y. Yu, W. Lu, Y. Liu, and H. Zhu, "Measurement and modeling of wireless off-body propagation characteristics under hospital environment at 6-8.5 GHz," *IEEE Access*, vol. 5, pp. 10915–10923, May 2017.
[6] L. Xia, S. Redfield, and P. Chiang, "Experimental characterization of a UWB channel for body area networks," *EURASIP J. Wireless Commun. Netw.*, vol. 2011, no. 1, pp. 1–11, Jan. 2011.
[7] S. J. Ambroziak, L. M. Correia, R. J. Katulski, M. Mackowiak, C. Oliveira, J. Sadowski, and K. Turbic, "An off-body channel model for body area networks in indoor environments," *IEEE Trans. Antennas Propag.*, vol. 64, no. 9, pp. 4022–4035, Sep. 2016.
[8] H. Kdouh, C. Brousseau, G. Zaharia, G. Grunfelder, and G. E. Zein, "Measurements and path loss models for shipboard environments at 2.4 GHz," in *Proc. 41st Eur. Microw. Conf.*, Manchester, U.K., Oct. 2011, pp. 408–411.
[9] A. Mariscotti, M. Sassi, A. Qualizza, and M. Lenardon, "On the propagation of wireless signals on board ships," in *Proc. IEEE Instrum. Meas. Technol. Conf.*, Austin, TX, USA, May 2010, pp. 1418–1423.
[10] X. H. Mao, Y. H. Lee, and B. C. Ng, "Wideband channel characterization along a lift shaft on board a ship," in *Proc. IEEE Antennas Propag. Soc. Int. Symp.*, Toronto, ON, Canada, Jul. 2010, pp. 1–4.
[11] E. Balboni, J. Ford, R. Tingley, K. Toomey, and J. Vytal, "An empirical study of radio propagation aboard naval vessels," in *Proc. IEEE-APS Conf. Antennas Propag. Wireless Commun.*, Waltham, MA, USA, Nov. 2000, pp. 157–160.

[12] G. B. Tait and M. B. Slocum, "Electromagnetic environment characterization of below-deck spaces in ships," in *Proc. IEEE Int. Symp. Electromagn. Compat.*, Detroit, MI, USA, Aug. 2008, pp. 1–6.
[13] K. K. Cwalina, S. J. Ambroziak, P. Rajchowski, and L. M. Correia, "Radio channel measurements in 868 MHz off-body communications in a ferry environment," in *Proc. 32nd Gen. Assem. Sci. Symp. Int. Union Radio Sci. (URSI GASS)*, Montreal, QC, Canada, Aug. 2017, pp. 1–4.
[14] F. D. Cardoso, P. T. Kosz, M. M. Ferreira, S. J. Ambroziak, and L. M. Correia, "Fast fading characterization for body area networks in circular metallic indoor environments," *IEEE Access*, vol. 8, pp. 43817–43825, Mar. 2020.
[15] C. Roblin, "Analysis of the channel power delay profile of WBAN scenarios in various indoor environments," in *Proc. IEEE Int. Conf. Ultra-Wideband (ICUWB)*, Bologna, Italy, Sep. 2011, pp. 545–549.
[16] K. Turbic, S. J. Ambroziak, L. M. Correia, and M. Beko, "Wideband off-body channel characteristics with dynamic user," in *Proc. 13th Eur. Conf. Antennas Propag. (EuCAP)*, Krakow, Poland, Mar. 2019, pp. 1–2.
[17] E. Reusens, W. Joseph, B. Latre, B. Braem, G. Vermeeren, E. Tanghe, L. Martens, I. Moerman, and C. Blondia, "Characterization of on-body communication channel and energy efficient topology design for wireless body area networks," *IEEE Trans. Inf. Technol. Biomed.*, vol. 13, no. 6, pp. 933–945, Nov. 2009.
[18] G. Glaeser, "Reflections on spheres and cylinders of revolution," *J. Geometry Graph.*, vol. 3, no. 2, pp. 121–139, 1999.
[19] E. H. Lockwood, *A Book of Curves*. Cambridge, U.K.: Cambridge Univ. Press, 1961.
[20] J. Hejselbæk, A. Karstensen, J. Nielsen, W. Fan, and G. F. Pedersen, "Validation of emulated omnidirectional antenna output using directive antenna data," in *Proc. 11th Eur. Conf. Antennas Propag. (EuCAP)*, Paris, France, Mar. 2017, pp. 131–135.
[21] J. D. Parsons, *The Mobile Radio Propagation Channel*. Chichester, U.K.: Wiley, 2000.
[22] M. J. Evans and J. S. Rosenthal, *Probability and Statistics: The Science of Uncertainty*, 2nd, ed. New York, NY, USA: W.H. Freeman, 2009.
[23] T. S. Rappaport, *Wireless Communications Principles and Practice*. Upper Saddle River, NJ, USA: Prentice-Hall, 2002.

FILIPE D. CARDOSO (Member, IEEE) received the Licenciado, M.Sc., and Ph.D. degrees in electrical and computer engineering from the IST/Technical University of Lisbon. Since 1994, he has been with the Department of Electrical Engineering, ESTSetúbal/Polytechnic Institute of Setúbal, Portugal, where he is currently a Tenured Professor in telecommunications and the Head of the electronics and telecommunications area. He is also a Researcher with INESC-ID, Lisbon. He is also involved in European projects and networks of excellence COST 273, IST/FLOWS, ICT/4WARD, ICT/EARTH, ICT/LEXNET, NEWCOM, and NEWCOM++. He was a Task Leader of Energy Efficiency in Transmission Techniques (EARTH) and Dissemination and Standardization (LEXNET) workgroups. He has authored papers in national and international conferences and journals, for which he has also served as a reviewer and a board member. He was a Secretary of the IEEE ComSoc Portuguese Chapter. His research interests include wireless/mobile channel characterization and modeling and future mobile broadband systems.

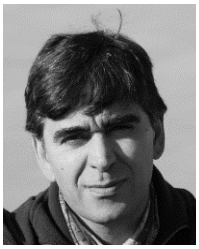

MANUEL M. FERREIRA received the Licenciado degree in electronics and telecommunications from the University of Aveiro and the M.Sc. degree in electrical and computer engineering from the IST/Technical University of Lisbon. Since 1995, he has been with the Department of Electrical Engineering, ESTSetúbal/Polytechnic Institute of Setúbal, Portugal. He was involved in European projects and networks of excellence NEWCOM and ICT/LEXNET. His research interests include wireless/mobile channel characterization and wireless sensor networks.

SŁAWOMIR J. AMBROZIAK (Senior Member, IEEE) was born in Poland, in 1982. He received the M.Sc., Ph.D., and D.Sc. degrees in radio communication from the Gdańsk University of Technology (GUT), Poland, in 2008, 2013, and 2020, respectively. Since 2008, he has been with the Department of Radiocommunication Systems and Networks, GUT, from 2008 to 2013, as a Research Assistant; from 2013 to 2020, as an Assistant Professor; and since 2020, as an Associate Professor. He is the author or coauthor of many publications, including book, book chapters, articles, reports, and papers presented during international and domestic conferences. He participated and still participates in several projects related to special application of wireless techniques and two COST Actions (IC1004 and CA15104). His main scope of research is radio channel modelling in body area networks. His research interests include wireless communication and radio wave propagation. He is a Senior Member of URSI and a member of Gdańsk Scientific Society. He is also a member of the Board of the Working Group on Propagation of the European Association on Antennas and Propagation (EurAAP), Management Committee Substitute Member of the COST CA15104 Action. He was a recipient of the Young Scientists Awards of URSI, in 2016 and 2011, the Eighth International Conference on Wireless and Mobile Communications Best Paper Award, in 2012, and many domestic awards. He is also the Chair of the Sub Working Group Internet-of-Things for Health, and the Vice-Chair of Commission-F of the Polish National Committee of URSI.

LUIS M. CORREIA (Senior Member, IEEE) was born in Portugal, in 1958. He received the Ph.D. degree in electrical and computer engineering from IST (known as University of Lisbon) in 1991. He is currently a Professor in telecommunications with IST, with his work focused on wireless and mobile communications, with the research activities developed in the INESC-ID Institute. He has acted as a Consultant for the Portuguese telecommunications operators and regulator, besides other public and private entities, and has been in the board of directors of a telecommunications company. He has participated in 32 projects within European frameworks, having coordinated six, and taken leadership responsibilities at various levels in many others, besides national ones. He has supervised over 220 M.Sc./Ph.D. students, having edited six books, contribute to European strategic documents, and authored over 500 papers in international and national journals and conferences, for which served also as a reviewer, editor, and board member. Internationally, he was a part of 37 Ph.D. juries, 71 research projects and institutions evaluation committees for funding agencies in 12 countries, and the European Commission and COST. He has been the Chairman of Conference of the Technical Program Committee and the steering committee of various major conferences, besides other several duties. He was a National Delegate to the COST Domain Committee on ICT. He has launched and served as the Chairman of the IEEE Communications Society Portugal Chapter. He is an Honorary Professor of the Gdańsk University of Technology, Poland. He was a recipient of the 2021 EurAAP Propagation Award for leadership in the field of propagation for wireless and mobile communications.